

Crystal Structure and Properties of the Rare-Earth-Metal Rhodium Carbides $R_8Rh_5C_{12}$ ($R = Y, Gd-Tm$)

Rolf-Dieter Hoffmann, Wolfgang Jeitschko,* Manfred Reehuis, and Stephen Lee†

Received June 1, 1988

The title compounds were obtained by arc melting of the elements. They are also thermodynamically stable at 900 °C. Their crystal structure is monoclinic, space group $C2/m$ with $Z = 2$ formula units per cell. It was determined from single-crystal X-ray data for $Er_8Rh_5C_{12}$, which has the lattice constants $a = 2772.6$ (3) pm, $b = 349.09$ (4) pm, $c = 729.8$ (1) pm, and $\beta = 94.17$ (1)°. The full-matrix least-squares refinement resulted in a conventional residual of $R = 0.031$ for 1868 structure factors and 73 variable parameters. The structure contains a finite chainlike centrosymmetric polyanion $[Rh_5C_{12}]^{24-}$ with two Rh-Rh bonds (270.8 pm) and six pairs of carbon atoms (C-C bond lengths: 127, 132, 133 pm). The hydrolysis with 2 N hydrochloric acid yields mainly methane, ethane, propane, and *n*-butane but no unsaturated hydrocarbons. $Y_8Rh_5C_{12}$ is a metallic conductor but does not become superconducting above 1.9 K. Magnetic susceptibility measurements of $Y_8Rh_5C_{12}$ show temperature-dependent weak paramagnetism, while the other $Er_8Rh_5C_{12}$ -type compounds are Curie-Weiss paramagnetic with magnetic moments corresponding to those of the rare-earth-metal ions.

Introduction

The ternary systems of the rare-earth elements with iron or cobalt and carbon contain numerous ternary carbides.¹ Structure determinations were reported for $CeCoC_2$,² $DyCoC_2$,³ $ScCoC_2$,⁴ Sc_3CoC_4 ,⁵ $YCoC_4$,⁶ Y_2FeC_4 ,⁷ and Er_2FeC_4 .⁷ Very little is known about homologous carbides with the platinum metals.⁸ We have recently started to investigate such systems and briefly reported already on $Er_8Rh_5C_{12}$ ⁹ and $Er_{10}Ru_{10}C_{19}$.¹⁰ Here we give a full account of our experimental work on the $Er_8Rh_5C_{12}$ -type compounds. Chemical bonding in these compounds will be treated in a further paper.¹¹

Sample Preparation and Lattice Constants

Turnings of the rare-earth metals (nominal purity >99.9%), rhodium powder (>99.9%, 240 mesh), and graphite flakes (99.5%) were used as starting materials. The samples were prepared by arc-melting cold-pressed pellets of the ideal elemental 8:5:12 mixtures in an atmosphere of argon (99.996%), which was further purified by melting a titanium button prior to the reactions. For the annealing in evacuated silica tubes (10-15 days at 900 °C) the samples were wrapped in tantalum foil. They were subsequently quenched in cold water. Only minor amounts (up to about 3%) of second- and/or third-phase products were observed in the Guinier powder patterns of the Gd, Dy, and Ho phases. No impurity phases were detected in the other samples. Energy-dispersive analyses in a scanning electron microscope did not reveal any impurity element heavier than magnesium.

The Guinier patterns were recorded with $Cu K\alpha_1$ radiation and α -quartz ($a = 491.30$ pm, $c = 540.46$ pm) as a standard. Indices were assigned on the basis of the monoclinic *C*-centered cell found from the single-crystal work on $Er_8Rh_5C_{12}$ by using the intensities of the calculated patterns¹² for guidance. The evaluation of the powder pattern of $Y_8Rh_5C_{12}$ is shown as an example in Table I. Table II lists the lattice constants obtained by least-squares fits of the data. The plot of the cell volumes (Figure 1) shows the expected lanthanoid contraction.

Chemical Properties

In contrast to the binary rare-earth-metal carbides, the ternary rhodium-containing carbides $R_8Rh_5C_{12}$ are stable in air for some time, especially if they are well crystallized. The powdered samples, however, show serious signs of deterioration after several months. The gaseous products of the hydrolysis of $Er_8Rh_5C_{12}$ with 2 N hydrochloric acid at room temperature were analyzed in a gas chromatograph by a flame ionization detector. Besides hydrogen (which was not measured), the hydrolysis products consisted mainly of the following hydrocarbons (in wt %): 45, CH_4 ; 30, C_2H_6 ; 10, C_3H_8 ; 13, $n-C_4H_{10}$. Minor amounts of *i*- C_4H_{10} and the various isomers of pentane and hexane were also detected. Thus, even though the structure determination shows that the C-C bond distances of the C_2 pairs are close to those of double bonds, no unsaturated hydrocarbons were observed, in contrast to the

results for related carbides under similar conditions.^{3,6,7,13,14}

Electrical Conductivity and Magnetic Properties

The crystals of the ternary carbides are gray with a metallic luster. The temperature dependence of the electrical conductivity was determined for a small piece ($250 \times 75 \times 25 \mu m^3$) of an ingot of $Y_8Rh_5C_{12}$ contacted with indium solder. $Y_8Rh_5C_{12}$ is a metallic conductor. Its conductivity decreased smoothly by a factor of 1.36 on heating from 298 to 554 K. At 25 °C the specific resistivity was $\rho = 0.6 \times 10^{-3} \Omega\text{-cm}$. As a probe for superconductivity, we determined the ac inductivity of $Y_8Rh_5C_{12}$ at low temperature. Such a transition was not found above 1.9 K.

The magnetic susceptibilities were determined with a Faraday balance for samples of about 10 mg in a magnetic field of 1 T. The absence of ferromagnetic impurities was ascertained by the absence of a magnetic field dependence of the susceptibilities.

$Y_8Rh_5C_{12}$ is weakly paramagnetic with some temperature dependence. At room temperature a susceptibility of $\chi = 43$ (2) $\times 10^{-6} \text{ cm}^3/\text{formula unit (fu)}$ was obtained. It increased to a value of $\chi = 683$ (50) $\times 10^{-6} \text{ cm}^3/\text{fu}$ at 75 K. With a correction for the core diamagnetism (computed from the increments,¹⁵ where the increment for the C-C double bond is certainly problematic in a metallic solid) of $\chi_c = -352 \times 10^{-6} \text{ cm}^3/\text{fu}$, the $1/\chi$ vs T plot is approximately linear within this temperature range, suggesting Curie-Weiss behavior (with a paramagnetic Curie temperature of about -110 K). However, considering the large formula unit, the magnetic moment computed from the slope of this line is small: $\mu_{\text{exp}} = 1.3 \mu_B$. In view of the metallic conductivity, we ascribe this behavior to a weak interaction between the itinerant electrons.

$Tb_8Rh_5C_{12}$ and $Ho_8Rh_5C_{12}$ show Curie-Weiss-type paramagnetic behavior. The effective magnetic moments per lanthanoid

- (1) Stadelmaier, H. H.; Park, H. K. *Z. Metallkd.* **1981**, *72*, 417. Park, H. K.; Stadelmaier, H. H.; Jordan, L. T. *Z. Metallkd.* **1982**, *73*, 399.
- (2) Stadelmaier, H. H.; Liu, N.-Ch. *Z. Metallkd.* **1985**, *76*, 585.
- (3) Bodak, O. I.; Marusin, E. P.; Bruskov, V. A. *Sov. Phys.—Crystallogr. (Engl. Transl.)* **1980**, *25*, 355.
- (4) Jeitschko, W.; Gerss, M. H. *J. Less-Common Met.* **1986**, *116*, 147.
- (5) Marusin, E. P.; Bodak, O. I.; Tsokol', A. O.; Baivel'man, M. G. *Sov. Phys.—Crystallogr. (Engl. Transl.)* **1985**, *30*, 340.
- (6) Tsokol', A. O.; Bodak, O. I.; Marusin, E. P. *Sov. Phys.—Crystallogr. (Engl. Transl.)* **1986**, *31*, 466.
- (7) Gerss, M. H.; Jeitschko, W. *Z. Naturforsch., B* **1986**, *41*, 946.
- (8) Gerss, M. H.; Jeitschko, W.; Boonk, L.; Nientiedt, J.; Grobe, J.; Mörsen, E.; Leson, A. *J. Solid State Chem.* **1987**, *70*, 19.
- (9) Holleck, H. *Binäre und ternäre Carbide- und Nitridsysteme der Übergangsmetalle*; Gebrüder Borntraeger: Berlin, Stuttgart, 1984.
- (10) Hoffmann, R.-D.; Jeitschko, W. *Z. Kristallogr.* **1986**, *174*, 85.
- (11) Hoffmann, R.-D.; Jeitschko, W. *Z. Kristallogr.* **1987**, *178*, 110.
- (12) Lee, S.; Jeitschko, W.; Hoffmann, R.-D. *Inorg. Chem.*, submitted for publication.
- (13) Yvon, K.; Jeitschko, W.; Parthé, E. *J. Appl. Crystallogr.* **1977**, *10*, 73.
- (14) Gerss, M. H.; Jeitschko, W. *Mater. Res. Bull.* **1986**, *21*, 209.
- (15) Gerss, M. H.; Jeitschko, W. *Z. Kristallogr.* **1986**, *175*, 203.
- (16) Weiss, A.; Witte, H. *Magnetochemie*; Verlag Chemie: Weinheim, FRG, 1972.

† Alexander von Humboldt scholar. Present address: Department of Chemistry, University of Michigan, Ann Arbor, MI 48109.

Table I. Guinier Powder Pattern of $Y_8Rh_5C_{12}$ ^a

| <i>hkl</i> | Q_o | Q_c | I_o | I_c | <i>hkl</i> | Q_o | Q_c | I_o | I_c | <i>hkl</i> | Q_o | Q_c | I_o | I_c |
|------------|-------|-------|-------|-------|------------|-------|-------|-------|-------|------------|--------|---------|-------|-------|
| 200 | 52 | 52 | 20 | 25 | 312 | 1695 | 1696 | 20 | 42 | 114 | | 3799 | | 9 |
| 001 | 187 | 185 | 5 | 3 | -4,0,3 | 1796 | 1796 | 30 | 22 | -3,1,4 | 3811 | 3801 | 30 | 7 |
| 400 | 207 | 207 | 30 | 29 | -5,1,2 | | 1801 | 1801 | | 4 | | -15,1,1 | | 3807 |
| -2,0,1 | 224 | 224 | 30 | 21 | 910 | 1850 | 1851 | 30 | 27 | -6,2,1 | 3815 | | | 1 |
| -4,0,1 | 367 | 367 | 20 | 9 | 12,0,0 | 1867 | 1867 | 20 | 16 | -11,1,3 | 3823 | | | 13 |
| 600 | 467 | 467 | 20 | 10 | -10,0,2 | 1907 | 1908 | 40 | 32 | 13,1,2 | 3892 | 3898 | 5 | 7 |
| -6,0,1 | 614 | 613 | 5 | 3 | 512 | 1929 | 1929 | 11 | | -14,0,3 | 3938 | 3937 | 5 | 3 |
| 110 | 816 | 814 | 30 | 3 | 403 | 1951 | 1949 | 10 | 24 | 804 | 3995 | 3995 | 5 | 4 |
| 202 | | 818 | | 11 | -9,1,1 | 1979 | 1978 | 10 | 11 | 15,1,1 | 4000 | 3999 | 5 | 2 |
| -4,0,2 | 894 | 896 | 40 | 39 | -7,1,2 | 2086 | 2086 | 30 | 14 | -10,0,4 | 4000 | 4000 | | 3 |
| -8,0,1 | 964 | 964 | 30 | 11 | 603 | 2246 | 2247 | 30 | 23 | -4,2,2 | 4099 | 4098 | 5 | 11 |
| -1,1,1 | 997 | 992 | 30 | 7 | 712 | 2265 | 2266 | 30 | 17 | 18,0,0 | 4201 | 4201 | | 2 |
| 402 | | 999 | | 15 | -8,0,3 | 2341 | 2341 | 10 | 10 | 422 | 4201 | 10 | 5 | |
| 111 | 1005 | 1005 | 3 | 3 | -9,1,2 | 2474 | 2475 | 20 | 18 | 514 | 4213 | 4213 | | 12 |
| -3,1,1 | 1082 | 1083 | 30 | 21 | -3,1,3 | 2526 | 2525 | 10 | 13 | -7,1,4 | 4217 | 4217 | | 3 |
| 311 | 1125 | 1121 | 60 | 0 | -5,1,3 | 2693 | 2694 | 10 | 7 | -15,1,2 | 4265 | 4265 | | 8 |
| 510 | | 1125 | | 42 | 12,0,2 | 2770 | 2761 | 5 | 3 | -13,1,3 | 4405 | 4407 | 20 | 19 |
| -6,0,2 | 1130 | 1130 | 4 | 4 | -10,0,3 | 2769 | 2769 | 3 | 3 | 10,2,0 | 4497 | 4499 | 20 | 17 |
| 10,0,0 | 1297 | 1296 | 60 | 48 | 14,0,1 | 2816 | 2816 | 10 | 17 | 17,1,0 | 4546 | 4547 | 20 | 30 |
| 511 | 1342 | 1342 | 60 | 50 | 004 | 2960 | 2960 | 20 | 3 | -9,1,4 | 4580 | 4580 | | 11 |
| -10,0,1 | 1418 | 1417 | 10 | 17 | -2,0,4 | 2961 | 2961 | 10 | 8 | -10,2,1 | 4620 | 4620 | | 7 |
| 710 | 1435 | 1436 | 100 | 100 | -14,0,2 | 3102 | 3102 | 10 | 8 | -17,1,1 | 4622 | 4623 | 10 | 6 |
| -1,1,2 | 1542 | 1541 | 5 | 14 | 10,0,3 | 3154 | 3154 | 11 | 11 | 005 | 4625 | 4625 | | 1 |
| 112 | 1567 | 1566 | 60 | 61 | 020 | 3202 | 3202 | 40 | 55 | -4,0,5 | 4701 | 4705 | 10 | 3 |
| -7,1,1 | 1576 | 1576 | 7 | 7 | 13,1,1 | 3261 | 3260 | 10 | 4 | -18,0,2 | 4710 | 4710 | 10 | 2 |
| -3,1,2 | 1617 | 1619 | 100 | 98 | -16,0,1 | 3402 | 3401 | 5 | 5 | 023 | 4870 | 4867 | 10 | 3 |
| 003 | 1666 | 1665 | 60 | 7 | 14,0,2 | 3464 | 3461 | 5 | 8 | 822 | 4874 | 4874 | 10 | 12 |
| 711 | | 1666 | | 53 | | | | | | | 13,1,3 | 4907 | 4907 | 10 |
| 802 | 1672 | 1672 | 27 | 27 | | | | | | -4,2,3 | 5001 | 4998 | 5 | 11 |

^aThe diagram was recorded with Cu $K\alpha_1$ radiation. The Q values are defined by $Q = 100/d^2$ (nm⁻²). For the intensity calculation the positional parameters of $Er_8Rh_5C_{12}$ were used. Because of the large number of reflections, only those with $I_c \geq 7$ and all observed reflections are listed.

Table II. Cell Dimensions of Monoclinic $Er_8Rh_5C_{12}$ -Type Compounds^a

| compd | <i>a</i> , pm | <i>b</i> , pm | <i>c</i> , pm | β , deg | <i>V</i> , nm ³ |
|------------------|---------------|---------------|---------------|---------------|----------------------------|
| $Y_8Rh_5C_{12}$ | 2783.0 (3) | 353.51 (4) | 736.67 (9) | 93.74 (1) | 0.7232 (6) |
| $Gd_8Rh_5C_{12}$ | 2791.5 (4) | 360.31 (6) | 745.3 (1) | 93.28 (2) | 0.7484 (8) |
| $Tb_8Rh_5C_{12}$ | 2780.4 (6) | 356.82 (8) | 739.8 (2) | 93.53 (3) | 0.7326 (8) |
| $Dy_8Rh_5C_{12}$ | 2779.1 (4) | 354.09 (7) | 736.6 (1) | 93.80 (2) | 0.7233 (8) |
| $Ho_8Rh_5C_{12}$ | 2774.3 (3) | 351.58 (5) | 733.4 (1) | 94.00 (1) | 0.7135 (7) |
| $Er_8Rh_5C_{12}$ | 2772.6 (3) | 349.09 (4) | 729.8 (1) | 94.17 (1) | 0.7045 (7) |
| $Tm_8Rh_5C_{12}$ | 2766.6 (3) | 346.74 (6) | 726.8 (1) | 94.36 (1) | 0.6952 (9) |

^aStandard deviations in the least significant digits are given in parentheses.

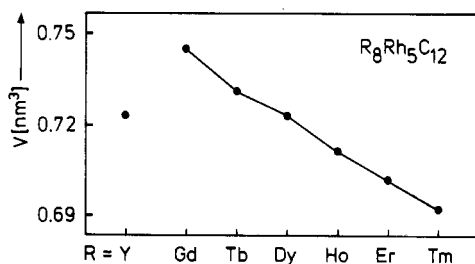


Figure 1. Cell volumes of the $Er_8Rh_5C_{12}$ -type carbides. The size of the dots approximately corresponds to the standard deviations.

ion μ_{exp} were determined from the linear slopes of the $1/\chi$ vs T plots, which we could extrapolate to $T = 0$ K for $1/\chi = 0$ (Figure 2). For the other $Er_8Rh_5C_{12}$ -type carbides we determined the susceptibilities only at room temperature and assumed similar behavior. The resulting magnetic moments are summarized in Table III. It can be seen that the experimentally determined effective magnetic moments correspond to those of the lanthanoid ions, albeit the experimental values are all slightly lower than the theoretical ones. Such small deviations from the ideal values were also observed for other rare-earth-metal compounds.¹⁶

Crystal Structure of $Er_8Rh_5C_{12}$

The single crystals of $Er_8Rh_5C_{12}$ used for the structure determination were isolated from a crushed arc-molten button with

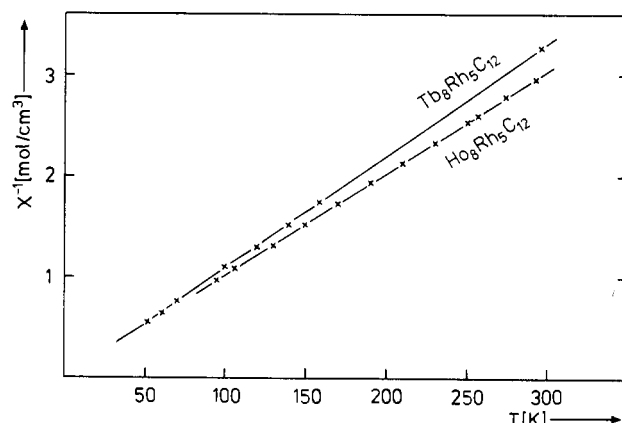


Figure 2. Reciprocal magnetic susceptibilities of $Tb_8Rh_5C_{12}$ and $Ho_8Rh_5C_{12}$ as a function of temperature.

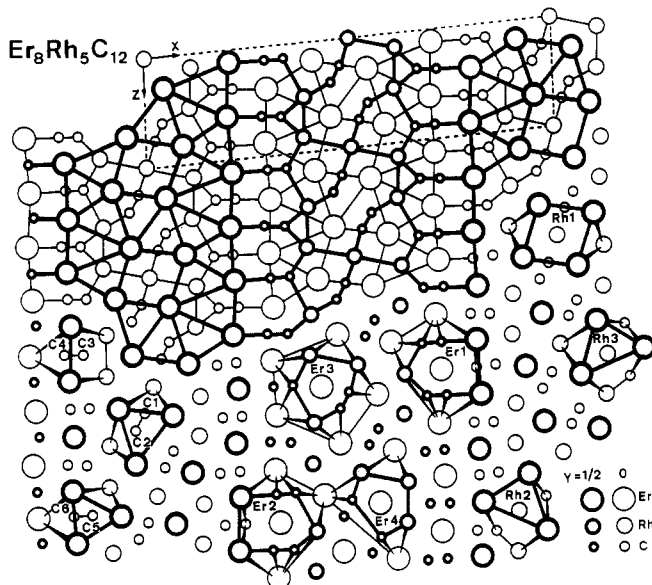
Table III. Effective Magnetic Moments per Lanthanoid Atom in Carbides with the $Er_8Rh_5C_{12}$ -Type Structure^a

| compd | μ_{exp} , μ_B | μ_{eff} , μ_B | compd | μ_{exp} , μ_B | μ_{eff} , μ_B |
|------------------|-----------------------|-----------------------|------------------|-----------------------|-----------------------|
| $Gd_8Rh_5C_{12}$ | 7.71 (5) | 7.94 | $Ho_8Rh_5C_{12}$ | 9.93 (9) | 10.60 |
| $Tb_8Rh_5C_{12}$ | 9.48 (7) | 9.72 | $Er_8Rh_5C_{12}$ | 9.16 (7) | 9.58 |
| $Dy_8Rh_5C_{12}$ | 10.08 (9) | 10.64 | $Tm_8Rh_5C_{12}$ | 7.22 (5) | 7.56 |

^aThe experimentally determined magnetic moments per lanthanoid atom μ_{exp} have error limits that are listed in parentheses in the place value of the least significant digit. They are compared to the effective moments calculated from the relation $\mu_{eff} = g[J(J+1)]^{1/2}$.

Table IV. Crystallographic Data for $\text{Er}_8\text{Rh}_5\text{C}_{12}$

| | |
|---------------------------------|---|
| lattice const: see Table II | $\rho_{\text{calcd}} = 9.41 \text{ g}\cdot\text{cm}^{-3}$ |
| $Z = 2$ | $\mu = 533 \text{ cm}^{-1}$ |
| fw = 1996.74 | transmission ratio |
| space group: $C2/m$ | (highest/lowest): 1.73 |
| (No. 12) | $R(F_o) = 0.031$ |
| $T = 21 \text{ }^\circ\text{C}$ | $R_w(F_o) = 0.027$ |
| $\lambda = 0.7107 \text{ \AA}$ | |

**Figure 3.** Crystal structure and coordination polyhedra of $\text{Er}_8\text{Rh}_5\text{C}_{12}$. Atoms connected by thin and thick lines are at different heights of the projection direction.

the initial atomic composition $\text{Er}:\text{Rh}:\text{C} = 33:26:41$. Bürger precession and Weissenberg diffractograms showed the Laue symmetry $2/m$. The extinction conditions (reflections hkl were observed only for $h+k=2n$) led to the space groups $C2$, Cm , and $C2/m$, of which the centrosymmetric group $C2/m$ was found to be correct during the structure determination. The crystallographic data are summarized in Table IV and in a more detailed table in the supplementary material.

The intensity data were collected from a crystal of dimensions $5 \times 10 \times 40 \mu\text{m}^3$ in an automated four-circle diffractometer with graphite-monochromated $\text{Mo K}\alpha$ radiation by $\theta/2\theta$ -scans in the whole reciprocal space up to $2\theta = 90^\circ$. An empirical absorption correction was made from ψ -scan data.

The structure was determined from Patterson and difference Fourier syntheses. It was refined by full-matrix least-squares cycles using a program system supplied by the Enraf-Nonius company. The atomic scattering factors¹⁷ were corrected for anomalous dispersion.¹⁸ Weights were assigned according to the counting statistics ($w = 1/\sigma_{F^2}$). A parameter accounting for an isotropic secondary extinction was refined and applied to the calculated structure factors. As a check for the ideal composition, we fixed the scale factor and varied the occupancy parameters of all atoms along with their thermal parameters. All occupancy parameters were within five standard deviations of the ideal composition, and thus one may assume the ideal occupancies, especially also for the carbon atoms, where a large percentage of defects is found in some structures.¹⁹ However, since the occupancy parameters of all erbium atoms were all slightly greater and those of the rhodium atoms were all slightly smaller than the ideal values, we preferred to consider these least-squares cycles as the final ones. Nevertheless, this regularity may be accidental and we will not discuss it any further at this time. The final conventional residual is $R = 0.031$ ($R_w = 0.027$) for 73 variable

Table V. Atomic Parameters of $\text{Er}_8\text{Rh}_5\text{C}_{12}$ ^a

| atom | $C2/m$ | occupancy | x | y | z | B |
|-------|--------|-----------|-------------|-----|-------------|-----------|
| Er(1) | 4i | 1.004 (2) | 0.29360 (2) | 0 | 0.88381 (6) | 0.370 (6) |
| Er(2) | 4i | 1.004 (2) | 0.30038 (2) | 0 | 0.39119 (6) | 0.391 (6) |
| Er(3) | 4i | 1.002 (2) | 0.41225 (2) | 0 | 0.17097 (7) | 0.499 (6) |
| Er(4) | 4i | 1.010 (2) | 0.45305 (2) | 0 | 0.70235 (7) | 0.700 (7) |
| Rh(1) | 2a | 0.991 (4) | 0 | 0 | 0 | 0.66 (2) |
| Rh(2) | 4i | 0.999 (3) | 0.11105 (2) | 0 | 0.4978 (1) | 0.69 (1) |
| Rh(3) | 4i | 0.995 (3) | 0.11565 (3) | 0 | 0.1284 (1) | 0.60 (1) |
| C(1) | 4i | 0.88 (3) | 0.0226 (4) | 0 | 0.755 (1) | 0.4 (1) |
| C(2) | 4i | 0.94 (3) | 0.0461 (4) | 0 | 0.612 (2) | 0.7 (1) |
| C(3) | 4i | 0.91 (3) | 0.1689 (4) | 0 | 0.347 (1) | 0.3 (1) |
| C(4) | 4i | 0.99 (3) | 0.2167 (4) | 0 | 0.364 (1) | 0.5 (1) |
| C(5) | 4i | 1.04 (4) | 0.1588 (5) | 0 | 0.870 (2) | 1.2 (2) |
| C(6) | 4i | 0.99 (3) | 0.2067 (4) | 0 | 0.868 (1) | 0.4 (1) |

^aNumbers in parentheses are esd's in the least significant digits. The last column contains the isotropic B values of the carbon positions and the equivalent isotropic B values ($\times 100$, in units of nm^2) of the anisotropic temperature parameters of the metal positions.

Table VI. Interatomic Distances (pm) in the Structure of $\text{Er}_8\text{Rh}_5\text{C}_{12}$ ^a

| | | | |
|-------------|------------|-------------|------------|
| Er(1)-1C(6) | 240.3 (10) | Rh(1)-2C(1) | 193.7 (11) |
| 2C(4) | 251.5 (7) | 4Er(4) | 300.8 (1) |
| 2C(6) | 251.7 (7) | 2Rh(3) | 327.4 (1) |
| 2C(3) | 268.9 (8) | 4Er(3) | 331.1 (1) |
| 2C(5) | 276.9 (9) | | |
| 2Rh(3) | 306.9 (1) | Rh(2)-1C(3) | 200.8 (10) |
| 2Er(1) | 349.1 (1) | 1C(2) | 203.8 (11) |
| 2Er(1) | 351.6 (1) | 1Rh(3) | 270.8 (1) |
| 1Er(2) | 361.3 (1) | 2Er(4) | 282.1 (1) |
| 2Er(2) | 362.0 (1) | 2Er(2) | 307.3 (1) |
| 1Er(2) | 369.3 (1) | 2Er(3) | 308.8 (1) |
| 1Er(3) | 377.0 (1) | | |
| | | Rh(3)-1C(3) | 209.6 (10) |
| Er(2)-1C(4) | 231.4 (10) | 1C(5) | 230.4 (12) |
| 2C(4) | 256.6 (7) | 1Rh(2) | 270.8 (1) |
| 2C(6) | 256.9 (7) | 2Er(3) | 285.8 (1) |
| 2C(3) | 267.8 (8) | 2Er(4) | 292.3 (1) |
| 2C(5) | 287.7 (10) | 2Er(1) | 306.9 (1) |
| 2Rh(2) | 307.3 (1) | 1Rh(1) | 327.4 (1) |
| 2Er(2) | 349.1 (1) | | |
| 1Er(3) | 359.6 (1) | C(1)-1C(2) | 126.9 (16) |
| 1Er(1) | 361.3 (1) | 1Rh(1) | 193.7 (11) |
| 2Er(1) | 362.0 (1) | 2Er(3) | 254.2 (8) |
| 1Er(1) | 369.3 (1) | 2Er(4) | 260.8 (8) |
| 2Er(2) | 374.4 (1) | | |
| | | C(2)-1C(1) | 126.9 (16) |
| Er(3)-2C(1) | 254.2 (8) | 1Rh(2) | 203.8 (11) |
| 2C(2) | 257.1 (8) | 2Er(3) | 257.1 (8) |
| 2C(5) | 263.3 (9) | 2Er(4) | 288.6 (9) |
| 2Rh(3) | 285.8 (1) | | |
| 2Rh(2) | 308.8 (1) | C(3)-1C(4) | 132.2 (14) |
| 2Rh(1) | 331.1 (1) | 1Rh(2) | 200.8 (10) |
| 2Er(3) | 349.1 (1) | 1Rh(3) | 209.6 (10) |
| 1Er(2) | 359.6 (1) | 2Er(2) | 267.8 (8) |
| 1Er(4) | 367.9 (1) | 2Er(1) | 268.9 (8) |
| 1Er(1) | 377.0 (1) | | |
| 1Er(4) | 378.2 (1) | C(4)-1C(3) | 132.2 (14) |
| 1Er(4) | 395.9 (1) | 1Er(2) | 231.4 (10) |
| | | 2Er(1) | 251.5 (7) |
| Er(4)-2C(1) | 260.8 (8) | 2Er(2) | 256.6 (7) |
| 2Rh(2) | 282.1 (1) | | |
| 2C(2) | 288.6 (9) | C(5)-1C(6) | 133.0 (16) |
| 2Rh(3) | 292.3 (1) | 1Rh(3) | 230.4 (12) |
| 2Rh(1) | 300.8 (1) | 2Er(3) | 263.3 (9) |
| 2Er(4) | 349.1 (1) | 2Er(1) | 276.9 (9) |
| 1Er(3) | 367.9 (1) | 2Er(2) | 287.7 (10) |
| 1Er(3) | 378.2 (1) | | |
| 1Er(3) | 395.9 (1) | C(6)-1C(5) | 133.0 (16) |
| | | 1Er(1) | 240.3 (10) |
| | | 2Er(1) | 251.7 (7) |
| | | 2Er(2) | 256.9 (7) |

^aAll distances shorter than 400 pm (Er-Er, Er-Rh), 340 pm (Rh-Rh), 320 pm (Er-C), and 290 pm (Rh-C, C-C) are listed. Standard deviations, computed from those of the lattice constants and the positional parameters, are given in parentheses.

(17) Cromer, D. T.; Mann, J. B. *Acta Crystallogr., Sect. A* **1968**, *24*, 321.(18) Cromer, D. T.; Liberman, D. *J. Chem. Phys.* **1970**, *53*, 1891.(19) Jeitschko, W.; Block, G. *Z. Anorg. Allg. Chem.* **1985**, *528*, 61. Block, G.; Jeitschko, W. *Inorg. Chem.* **1986**, *25*, 279. Block, G.; Jeitschko, W. *J. Solid State Chem.* **1987**, *70*, 271.

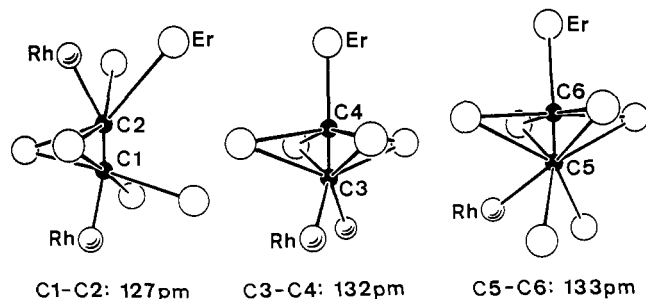


Figure 4. Near-neighbor environments of the C_2 pairs in $\text{Er}_8\text{Rh}_5\text{C}_{12}$.

parameters (the metal atoms with ellipsoidal and the carbon atoms with isotropic thermal parameters) and 1868 structure factors. The difference Fourier synthesis did not show any features at additionally possible atomic sites. The atomic parameters and interatomic distances are listed in Tables V and VI. The structure and the coordination polyhedra are shown in Figure 3. Listings of the anisotropic thermal parameters and of the calculated and observed structure factors are available as supplementary material.

Discussion

The structure of $\text{Er}_8\text{Rh}_5\text{C}_{12}$ represents a new structure type with three different kinds of C_2 pairs (Figure 4). The C-C bond distances of 127, 132, and 133 pm are between those of a triple (120 pm) and a double bond (134 pm) in hydrocarbons. They are among the shortest found so far in ternary carbides of the rare-earth metals and actinoids with transition metals. Other carbides of this kind include (with the C-C bond distances in units of picometers in parentheses) DyCoC_2 (137),³ DyNiC_2 (137),³ and SmRhC_2 (134)²⁰ with CeNiC_2 (141) type structure,²¹ CeCoC_2 (137)² and isotopic NdCoC_2 (140),²² and UCoC_2 (148),¹³ CeRhC_2 (141),²⁰ Sc_3CoC_4 (146),⁵ $\text{La}_2\text{Ni}_5\text{C}_3$ (136),^{22,23} Er_2FeC_4 (133),⁷ and U_2NiC_3 (143).¹⁴ The structures of ScCoC_2 ⁴ and $\text{La}_2\text{Re}_5\text{C}_{15}$ ²⁴ also contain C_2 pairs; however, their C-C bond distances of 126 (7) and 150 (10) pm have standard deviations too large to make them suited for comparisons. For the other ternary carbides the standard deviations are about 1 or 2 pm. Nevertheless, it seems difficult at this time to find a correlation between the C-C bond lengths and the composition of the carbides.

In this context it is of interest that the $\text{Er}_8\text{Rh}_5\text{C}_{12}$ structure contains slabs at $x = 1/4$ and $3/4$, which may be considered as cutouts of the CaC_2 -type structure. Accordingly, the C(4) and C(6) atoms of $\text{Er}_8\text{Rh}_5\text{C}_{12}$ have atomic environments that are virtually the same as those of the carbon atoms in the CaC_2 structure (if we substitute Ca atoms for the Er atoms). The distances of the bonds connecting the C(4) and C(6) atoms to the neighboring carbon atoms (132 and 133 pm) are somewhat larger than the C-C distances of about 129 pm in lanthanoid carbides with CaC_2 -type structure.²⁵ In the third C_2 pair of $\text{Er}_8\text{Rh}_5\text{C}_{12}$, where both carbon atoms have a rhodium neighbor, the C-C distance is shorter (127 pm).

If we count the interactions of the Er atoms with the Rh and C atoms as essentially ionic, we can write the formula as $[\text{Er}^{\text{III}}]_8^{24+}[\text{Rh}_5\text{C}_{12}]^{24-}$. The structure contains indeed a finite, chainlike, centrosymmetric Rh_5C_{12} cluster, which is shown in Figure 5. Its shortest distances to neighboring Rh_5C_{12} clusters are Rh-C distances of 294 pm and Rh-Rh distances of 327 pm. Thus, the Rh_5C_{12} units may be considered as separated from each other. The two Rh-Rh distances of 270.8 pm within the Rh_5C_{12} cluster on the other hand must be considered as bonding. They compare well with the Rh-Rh bonds of 266.5 pm in $\mu\text{-CH}_2[\eta\text{-C}_5\text{H}_5\text{Rh}(\text{CO})]_2$ ²⁶ and 272.3 pm in $[\{\text{RhFe}(\mu\text{-PPh}_2)_2(\mu\text{-CO})(\text{CO})_3\}_2]$.²⁷

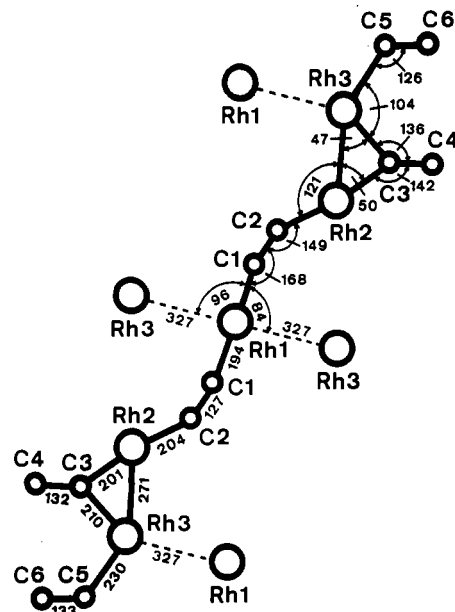


Figure 5. The polyanion $[\text{Rh}_5\text{C}_{12}]^{24-}$ of $\text{Er}_8\text{Rh}_5\text{C}_{12}$. All atoms of this centrosymmetric cluster are at the same height of the projection direction. Interatomic distances (pm) and angles (deg) are indicated in the lower and upper parts, respectively. The weak Rh(1)-Rh(3) interactions between adjacent $[\text{Rh}_5\text{C}_{12}]^{24-}$ polyanions are also shown.

They are also comparable to the *shortest* Rh-Rh bonds in polynuclear Rh clusters, e.g. 267.4 pm in $[\text{Rh}_{12}\text{C}_2(\text{CO})_{25}]$,²⁸ 269.9 pm in $[\text{Rh}_8(\text{CO})_{19}\text{C}]$,²⁹ 271.4 pm in $[\text{N}(\text{C}_3\text{H}_7)_4]_4[\text{Rh}_{12}\text{C}_2(\text{CO})_{23}]$,³⁰ 272.7 pm in $[\text{N}(\text{PPh}_3)_2]_2[\text{Rh}_{12}\text{C}_2(\text{CO})_{24}]$,³¹ 273.8 pm in $[\text{H}_3\text{O}][\text{Rh}_{15}(\text{CO})_{28}\text{C}_2]$,³² 277.6 pm in $[\text{NMe}_3(\text{CH}_2\text{Ph})]_2[\text{Rh}_6(\text{CO})_{15}\text{C}]$,³³ and 276.5 pm in $[\text{Cu}_2\text{Rh}_6(\text{CO})_{15}(\text{NCMe})_2] \cdot 0.5\text{MeOH}$,³⁴ while the *average* Rh-Rh bond distances in these polynuclear Rh clusters are greater and range between 278 and 283 pm in the compounds of ref 34 and 30, respectively.

The Rh-C distances of $\text{Er}_8\text{Rh}_5\text{C}_{12}$ cover the range from 194 to 231 pm. These values may be compared to the Rh-C single-bond value of 203 pm for the bonds connecting the Rh atoms to the bridging CH_2 groups in $\mu\text{-CH}_2[\eta\text{-C}_5\text{H}_5\text{Rh}(\text{CO})]_2$.²⁶ In the carbonyl carbide clusters enumerated above the average Rh-C bond lengths of terminal carbonyl groups range from 182 to 193 pm, while edge-bridging carbonyl groups have average Rh-C bond lengths of 203-212 pm. The mean Rh-C(carbide) distances in most of these clusters are between 212 and 214 pm. Thus, most Rh-C bonds in $\text{Er}_8\text{Rh}_5\text{C}_{12}$ have bond orders of about 1 and the Rh(1)-C(1) bond of 193 pm has some double-bond character, while the C(5) atoms at 231 pm can only be considered as weakly bonded to the Rh(3) atoms.

The polyanion $[\text{Rh}_5\text{C}_{12}]^{24-}$ has an odd number of electrons; nevertheless, the paramagnetism of $\text{Y}_8\text{Rh}_5\text{C}_{12}$ is weak and corresponds to less than one unpaired electron per formula unit. The magnetism of the other $\text{Er}_8\text{Rh}_5\text{C}_{12}$ -type compounds can be ascribed to that of the lanthanoid components. Chemical bonding in $\text{Er}_8\text{Rh}_5\text{C}_{12}$ will be analyzed in a forthcoming paper.¹¹ This analysis shows that the d states of the Rh atoms are essentially

- (20) Hoffmann, R.-D.; Jeitschko, W. *Z. Kristallogr.* **1988**, *182*, 137.
 (21) Bodak, O.-I.; Marusin, E. P. *Dopov. Akad. Nauk Ukr. RSR, Ser. A: Fiz.-Mat. Tekh. Nauki* **1979**, *12*, 1048.
 (22) Gerss, M. H.; Jeitschko, W. Unpublished results.
 (23) Tsokol', A. O.; Bodak, O. I.; Marusin, E. P. *Sov. Phys.-Crystallogr. (Engl. Transl.)* **1986**, *31*, 39.
 (24) Block, G.; Jeitschko, W. *Z. Kristallogr.* **1987**, *178*, 25.
 (25) Atoji, M. *J. Chem. Phys.* **1961**, *35*, 1950.
 (26) Herrmann, W. A.; Krüger, C.; Goddard, R.; Bernal, I. *Angew. Chem.* **1977**, *89*, 342; *Angew. Chem., Int. Ed. Engl.* **1977**, *16*, 334.

- (27) Haines, R. J.; Steen, N. D. C. T.; English, R. B. *J. Chem. Soc., Chem. Commun.* **1981**, 587.
 (28) Albano, V. G.; Chini, P.; Martinengo, S.; Sansoni, M.; Strumolo, D. *J. Chem. Soc., Dalton Trans.* **1978**, 459.
 (29) Albano, V. G.; Sansoni, M.; Chini, P.; Martinengo, S.; Strumolo, D. *J. Chem. Soc., Dalton Trans.* **1975**, 305.
 (30) Albano, V. G.; Braga, D.; Strumolo, D.; Seregni, C.; Martinengo, S. *J. Chem. Soc., Dalton Trans.* **1985**, 1309.
 (31) Albano, V. G.; Braga, D.; Chini, P.; Strumolo, D.; Martinengo, S. *J. Chem. Soc., Dalton Trans.* **1983**, 249.
 (32) Albano, V. G.; Chini, P.; Martinengo, S.; Sansoni, M.; Strumolo, D. *J. Chem. Soc., Chem. Commun.* **1974**, 299.
 (33) Albano, V. G.; Sansoni, M.; Chini, P.; Martinengo, S. *J. Chem. Soc., Dalton Trans.* **1973**, 651.
 (34) Albano, V. G.; Braga, D.; Martinengo, S.; Chini, P.; Sansoni, M.; Strumolo, D. *J. Chem. Soc., Dalton Trans.* **1980**, 52.

filled, in agreement with the almost nonmagnetic behavior of the Rh atoms. With the inclusion of the Er atoms, the Fermi level cuts through many bands. Thus, the metallic conductivity can be rationalized.

Acknowledgment. We are indebted to Dipl.-Chem. L. Boonk for the electrical conductivity measurements and for the superconductivity test of $Y_8Rh_5C_{12}$. We also thank Dr. M. H. Möller for the competent collection of the single-crystal diffractometer data, K. Wagner for the work on the scanning electron microscope, and Dipl.-Phys. Th. Vomhof for the magnetic characterization of $Y_8Rh_5C_{12}$. Dr. A. Ellmann, Dipl.-Chem. H. Ziemer, and Prof.

Dr. J. Grobe are thanked for help and advice with the gas chromatographic analysis. We also acknowledge Dr. R. Schwarz (Degussa AG) and Dr. G. Höfer (Heraeus Quarzschmelze) for generous gifts of rhodium metal and silica tubes. This work was supported by the Deutsche Forschungsgemeinschaft and the Fonds der Chemischen Industrie. Last but not least, we acknowledge the Alexander von Humboldt Foundation for a stipend to S.L.

Supplementary Material Available: Listings of the crystallographic data and the anisotropic thermal parameters for the metal atoms of $Er_8Rh_5C_{12}$ (1 page); a structure factor table (11 pages). Ordering information is given on any current masthead page.

Contribution from the Department of Chemistry, Rutgers, The State University of New Jersey, New Brunswick, New Jersey 08903, and Department of Inorganic and Analytical Chemistry, The Hebrew University, Jerusalem, Israel

Ru(2,2'-bpy)₂(NCS)₂X [X = CH₃CN, (CH₃)₂SO] and Related Compounds: Crystal Structure, VTFTIR, and NMR Study

R. H. Herber,*† Guijuan Nan,† J. A. Potenza,† H. J. Schugar,† and A. Bino†

Received September 7, 1988

The crystal structures of Ru(bpy)₂(NCS)₂, solvated with CH₃CN and (CH₃)₂SO, have been determined. Ru(C₁₀H₈N₂)₂(NC-S)₂·CH₃CN crystallizes in the monoclinic space group C2/c with $a = 10.230(2) \text{ \AA}$, $b = 15.209(3) \text{ \AA}$, $c = 16.186(2) \text{ \AA}$, $\beta = 105.19(1)^\circ$, $Z = 4$, and $R_F(R_{wp}) = 0.037(0.046)$ for 1023 reflections with $F_o^2 > 3\sigma(F_o^2)$; Ru(C₁₀H₈N₂)₂(NCS)₂·(CH₃)₂SO crystallizes in the triclinic space group P $\bar{1}$ with $a = 12.402(2) \text{ \AA}$, $b = 12.732(2) \text{ \AA}$, $c = 8.853(1) \text{ \AA}$, $\alpha = 105.70(3)^\circ$, $\beta = 103.06(2)^\circ$, $\gamma = 83.65(3)^\circ$, $Z = 2$, and $R_F(R_{wp}) = 0.053(0.068)$ for 3517 reflections with $F_o^2 > 3\sigma(F_o^2)$. In both complexes, the isothiocyanate ligands are cis. The CN absorbance in the IR spectra of the desolvated complex, as well as in the spectra of mulls of the DMSO-solvated material, has been determined and compared to those in the IR spectra of related cis and trans octahedral complexes of bis(isothiocyanate) species. The ¹³C NMR spectra in DMSO-*d*₆ show the expected 11 resonances associated with the cis configuration observed in the X-ray determinations. The implications of the spectroscopic signatures of these complexes in relation to their structures in the solid state and the extent to which these signatures are diagnostic with respect to the symmetry properties of these complexes are discussed.

Introduction

The chemistry of Ru(II) has received a great deal of attention in recent years, largely due to the richness of available oxidation states, large variability of ligand lability, and ease of coordination sphere modification available in ruthenium complexes.¹ Moreover, because of the great interest in determining the rate of electron transfer in biological systems, ruthenium complexes have been used as models for studying such processes on a rapid (nanosecond) time scale in a variety of chemical environments.²⁻⁶ In this latter context, variable-temperature Fourier transform infrared spectroscopy (VTFTIR) has proven to be a potentially fruitful method to examine the rate of electron transfer in mixed-valence compounds. This approach is predicated on the assumption that each metal center can be ligated with an appropriate "reporter" ligand, the IR signature of which will reflect the oxidation state and molecular level architecture of the metal center to which it is bonded. As has been discussed⁷ previously for a variety of inorganic and organometallic compounds, the thiocyanate and selenocyanate ligands can play the role of such a reporter group, and the detailed IR spectra of a large number of such compounds have been reported. Despite the fact that Ru(II) thiocyanates have been known^{8,9} for a number of years, no detailed structural studies, based on single-crystal X-ray diffraction data, have been reported, and the structural details of such compounds have been inferred indirectly from other (largely vibrational spectroscopic) data. In this context, a detailed VTFTIR study of rigorously desolvated Ru(2,2'-bpy)₂(NCS) has recently been reported.¹⁰ The observation of a single, symmetric absorbance in the CN stretching region, as well as an absorbance in the Raman spectrum at nearly the same frequency, has been interpreted as evidence for a trans configuration of the two pseudohalide groups, in contrast to the

cis configurations that have been assigned to the corresponding bis(chloro)¹¹ and bis(cyano) complexes.^{12,13} In the course of this IR study, it was observed that well-formed single crystals of the title compound could be recovered from CH₃CN and DMSO solutions. It has also proven feasible to examine the ¹H and ¹³C NMR spectra of the title compound in DMSO-*d*₆, as well as the infrared spectra of these solvated crystals in the presence of mother liquor. Finally, it has also proven possible to study the systematics of a number of related model compounds containing the SCN⁻ ligand. The details of these investigations are summarized in the present paper.

Experimental Section

(a) Preparation of Ru(2,2'-bpy)₂(NCS)₂·CH₃CN (1) and Ru(2,2'-bpy)₂(NCS)₂·(CH₃)₂SO (2). The parent aquo-solvated compound reported in this study was prepared by literature methods and characterized

- (1) Taube, H. *Comments Inorg. Chem.* **1981**, *1*, 17.
- (2) Callahan, R. W.; Keene, F. R.; Meyer, T. J.; Salmon, D. J. *J. Am. Chem. Soc.* **1977**, *99*, 1064.
- (3) Isied, S. S. *Prog. Inorg. Chem.* **1984**, *32*, 443.
- (4) Marcus, R. A.; Sutin, N. *Biochim. Biophys. Acta* **1985**, *811*, 265.
- (5) Mayo, S. L.; Ellis, W. R., Jr.; Crutchley, R. J.; Gray, H. B. *Science* **1986**, *233*, 948.
- (6) Plitzko, K.-D.; Boekelheide, V. *Angew. Chem., Int. Ed. Engl.* **1987**, *26*, 700.
- (7) Herber, R. H. *Rev. Silicon, Germanium, Tin Lead Compd.* **1986**, *9*, 113.
- (8) For a detailed review of the literature through 1983, see: Seddon, E. A.; Seddon, K. R. *The Chemistry of Ruthenium*; Elsevier, New York, 1984; and references therein.
- (9) Brandt, W. W.; Dwyer, F. P.; Gyarfas, E. C. *Chem. Rev.* **1954**, *54*, 959.
- (10) Herber, R. H.; Nan, G. *Inorg. Chem.* **1988**, *27*, 2644.
- (11) Bosnich, B.; Dwyer, F. P. *Aust. J. Chem.* **1966**, *19*, 2229. Goodwin, J. B.; Meyer, T. J. *Inorg. Chem.* **1971**, *10*, 471.
- (12) Demas, J. N.; Turner, T. F.; Crosby, G. A. *Inorg. Chem.* **1969**, *8*, 674.
- (13) Schilt, A. A. *Inorg. Chem.* **1964**, *3*, 1323.

* Rutgers University.

† The Hebrew University.